

THE NEAR-INFRARED SIZE-LUMINOSITY RELATIONS FOR HERBIG Ae/Be DISKS

J. D. MONNIER,¹ R. MILLAN-GABET,² R. BILLMEIER,¹ R. L. AKESON,² D. WALLACE,³ J.-P. BERGER,⁴ N. CALVET,⁵
P. D'ALESSIO,⁶ W. C. DANCHI,³ L. HARTMANN,⁵ L. A. HILLENBRAND,⁷ M. KUCHNER,⁸ J. RAJAGOPAL,³
W. A. TRAUB,⁵ P. G. TUTHILL,⁹ A. BODEN,² A. BOOTH,¹⁰ M. COLAVITA,¹⁰ J. GATHRIGHT,¹¹
M. HRYNEVYCH,¹¹ D. LE MIGNANT,¹¹ R. LIGON,¹⁰ C. NEYMAN,¹¹ M. SWAIN,¹⁰ R. THOMPSON,²
G. VASISHT,¹⁰ P. WIZINOWICH,¹¹ C. BEICHMAN,² J. BELETIC,¹¹ M. CREECH-EAKMAN,¹⁰
C. KORESKO,² A. SARGENT,² M. SHAO,¹⁰ AND G. VAN BELLE²

Received 2004 January 5; accepted 2005 January 28

ABSTRACT

We report the results of a sensitive K -band survey of Herbig Ae/Be disk sizes using the 85 m baseline Keck Interferometer. Targets were chosen to span the maximum range of stellar properties to probe the disk size dependence on luminosity and effective temperature. For most targets, the measured near-infrared sizes (ranging from 0.2 to 4 AU) support a simple disk model possessing a central optically thin (dust-free) cavity, ringed by hot dust emitting at the expected sublimation temperatures ($T_s \sim 1000$ – 1500 K). Furthermore, we find a tight correlation of disk size with source luminosity $R \propto L^{1/2}$ for Ae and late Be systems (valid over more than two decades in luminosity), confirming earlier suggestions based on lower quality data. Interestingly, the inferred dust-free inner cavities of the highest luminosity sources (Herbig B0–B3 stars) are *undersized* compared to predictions of the “optically thin cavity” model, likely because of optically thick gas within the inner AU.

Subject headings: accretion, accretion disks — circumstellar matter — instrumentation: interferometers — radiative transfer — stars: formation — stars: pre-main-sequence

Online material: color figure

1. INTRODUCTION

Young stellar objects (YSOs) are often observed to be surrounded by an optically thick accretion disk, presumably left over from early stages of star formation. These disks are expected to evolve into optically thin “debris” disks as the circumstellar material either accretes onto the central star, is blown out of the system, or coagulates into planetesimals. The disappearance of the optically thick protostellar accretion disk thus marks a transition between the final stages of star formation and the onset of planet formation. High angular resolution studies of these transition disks effectively test our physical models of accretion, as well as reveal the initial conditions for planet-building. In particular, infrared interferometers directly probe the temperature and density structure of gas and dust within the inner AU of YSO disks, critical ingredients in any recipe for planet formation.

Millan-Gabet et al. (1999) first discovered the marked discrepancy between theoretical predictions and the observed near-infrared (NIR) sizes of Herbig Ae/Be stars using the Infrared-Optical Telescope Array (IOTA) Interferometer—the AB Aur disk was

found to be many times larger than expected.¹² This pattern has been confirmed again and again, with “large” disk sizes for Herbig Ae/Be stars being found by Keck aperture masking (Tuthill et al. 2001; Danchi et al. 2001), additional IOTA work (Millan-Gabet et al. 2001), and Palomar Testbed Interferometer observations (Akeson et al. 2000, 2002; Eisner et al. 2003, 2004). More recently, a similar pattern has been found for bright T Tauri disks too (Akeson et al. 2000, 2005; Colavita et al. 2003).

Popular disk theories of that time (e.g., Lynden-Bell & Pringle 1974; Adams et al. 1987; Calvet et al. 1991; Hillenbrand et al. 1992; Hartmann et al. 1993; Chiang & Goldreich 1997) incorporated an optically thick, geometrically thin disk (with flaring, which is not so relevant for NIR wavelengths). In these models, the optically thick disk midplane shields inner dust from much of the stellar radiation, and thus hot dust near sublimation temperature ($T_s \sim 1500$ K) can exist quite close to the star. Interferometer measurements showed this emission to be much farther from the stars than these models predicted—thus arose the size controversy. About the same time, Natta et al. (2001) revisited the problem of the unrealistically high accretion rates inferred for some Herbig Ae/Be stars (on the basis of NIR excess; Hillenbrand et al. 1992; Hartmann et al. 1993) using spectroscopic observations from the *Infrared Space Observatory (ISO)*. These two observational “problems” would be resolved by the same solution.

First suggested by Tuthill et al. (2001) and independently developed by Natta et al. (2001) and Dullemond et al. (2001), the large disk sizes and excess NIR flux were naturally explained by the presence of an *optically thin* cavity surrounding the star. Thus, the innermost disk is *not* optically thick, presumably because dust, which is the primary source of opacity for $T \lesssim 1500$ K,

¹ University of Michigan Astronomy Department, 941 Dennison Building, Ann Arbor, MI 48109-1090; monnier@umich.edu.

² Michelson Science Center, California Institute of Technology, 770 South Wilson Avenue, Pasadena, CA 91125.

³ NASA Goddard Space Flight Center.

⁴ Laboratoire d’Astrophysique de Grenoble, 414 Rue de la Piscine, 38400 Saint Martin d’Heres, France.

⁵ Harvard-Smithsonian Center for Astrophysics, 60 Garden Street, Cambridge, MA 02138.

⁶ Universidad Nacional Autónoma de México.

⁷ Astronomy Department, California Institute of Technology, Pasadena, CA.

⁸ Princeton University, Princeton, NJ.

⁹ Physics Department, University of Sydney, Australia.

¹⁰ Jet Propulsion Laboratory, California Institute of Technology, 4800 Oak Grove Drive, Pasadena, CA 91109.

¹¹ W. M. Keck Observatory, California Association for Research in Astronomy, 65-1120 Mamalahoa Highway, Kamuela, HI 96743.

¹² In this paper, the “disk size” generally refers to the extent of the disk emission at a particular wavelength, not the *physical* extent of all the disk material.

is absent owing to evaporation by the stellar radiation field. This geometry explains the NIR excess flux as well since a frontally illuminated dust wall efficiently emits in the NIR. Interestingly, earlier modelers had already realized that the inner cavity would be devoid of dust because of the high temperatures (e.g., Hillenbrand et al. 1992), but the temperature profile adopted by these workers still implicitly incorporated an optically thick disk midplane. These central cavities are not necessarily devoid of gas; indeed, the optical depth of the gas depends on many factors (most notably, the accretion rate and geometry). Central clearings in YSO disks are not only interesting in the context of accretion disk physics but have been implicated in halting migration of the extrasolar hot Jupiter planets (Kuchner & Lecar 2002).

Monnier & Millan-Gabet (2002) put the “optically thin cavity” model to the most stringent test thus far by analyzing the full set of published interferometer measurements (including both T Tauri and Herbig Ae/Be stars for the first time) and found overall consistency through the use of a “size-luminosity” diagram. This diagram is particularly powerful because the inner radius of dust destruction is nearly independent of stellar temperature and almost a pure function of luminosity. This work also uncovered evidence for possible absorption by the *gaseous* inner disk of the most luminous sources in the sample, although interpretation was limited by significant data scatter due (at least in part) to the heterogeneous nature of the data sets.

Recently, Eisner et al. (2003, 2004) made significant contributions to the studies of these disks in a number of ways. First, they measured elongated NIR emission from some Herbig stars, evidence for disklike structure that had eluded the shorter baseline IOTA work. Furthermore, the size-luminosity relations of Monnier & Millan-Gabet (2002) were confirmed for the Herbig Ae stars. Perhaps most interestingly, Eisner et al. (2004) presented the clearest evidence to date for *undersized* disk emission around the early B stars in their sample. In fact, the NIR sizes of these disks were found consistent with the “classical” optically thick, geometrically thin disk models.

In this context, our group has carried out a survey of YSOs as part of “shared risk” commissioning of the Keck Interferometer. The Keck Interferometer boasts 10–100 times the sensitivity over previous-generation instruments, allowing a large number of Herbig Ae/Be, T Tauri, and FU Orionis objects to be targeted. In order to extend beyond existing work, we designed our survey as follows. First, great care was taken to choose targets with reliable spectral types and luminosities (early interferometers could detect relatively few targets and many had ambiguous classifications). Second, the greater instrumental sensitivity allowed us to probe systems spanning a larger range of spectral types and stellar luminosities.

Here we report our results for the Herbig Ae/Be portion of the survey, where we have significantly reduced the observational “scatter” that hampered previous studies. With the improved data quality, we can definitively characterize the size-luminosity relations of Herbig Ae/Be disks.

2. OBSERVATIONS

The Keck Interferometer (KI) was used during its visibility science commissioning period (2002–2004) to observe 14 Herbig Ae/Be stars as part of this survey (see Table 1). The KI is formed by two 10 m aperture telescopes (each consisting of 36 hexagonal mirror segments) separated by 85 m along a direction $\sim 38^\circ$ east of north, corresponding to a minimum fringe spacing of 5.3 mas at $2.2 \mu\text{m}$. In order to coherently combine the NIR light from such large apertures, each telescope utilizes a

natural guide star adaptive optics system (Wizinowich et al. 2003). Optical delay lines correct for sidereal motion and the telescope beams are combined at a beam splitter before the light is focused onto single-mode (fluoride) fibers which impose a ~ 50 mas (FWHM) field of view for all data reported herein. While both *H*- and *K*-band observations are now possible, only broad *K*-band ($2.18 \mu\text{m}$, $\Delta\lambda = 0.3 \mu\text{m}$) data are reported here. Owing to the large apertures and excellent site, the KI is currently the world’s most sensitive infrared interferometer, recently becoming the first such instrument to measure fringes on an extragalactic object (Swain et al. 2003). Further technical details can be found in recent KI publications (Colavita et al. 2003; Colavita & Wizinowich 2000, 2003).

Table 1 summarizes the basic properties of the target stars, including spectral type, distance, luminosity, and literature references for photometry used herein. Calibration of fringe data was performed by interspersing target observations with those of unresolved calibrators (see Table 2). The square of the fringe visibility (V^2) was measured using the ABCD method (using a dither mirror; see also Shao & Staelin 1977), and we followed the well-tested strategies described for the Palomar Testbed Interferometer (Colavita 1999), except that corrections for uneven telescope ratios were improved and jitter corrections were not applied. We refer the reader to Colavita et al. (2003) and Swain et al. (2003) for further description of calibration procedures.

The calibrated V^2 results appear in Table 3 along with the projected baseline (u , v) and date for each independent data set. The V^2 errors reported in this table only include statistical errors. Internal data quality checks have established a conservative upper limit to the systematic error $\Delta V^2 = 0.05$. Model fitting in this paper includes both sources of error in the uncertainty analysis.

3. METHODOLOGY

In this study, we wish to measure the characteristic NIR sizes of YSO accretion disks. By using a target sample spanning a wide range of stellar properties, we aim also investigate the size dependence on stellar luminosity. Interferometers have been successfully used to resolve stars since 1921 (Michelson & Pease 1921), and a full discussion of the methodology will not be given here. A single-baseline interferometer can effectively determine the characteristic size of an astronomical object by measuring the fringe “visibility,” a measure of the fringe contrast; unresolved sources produce high-contrast fringes (visibility unity), while resolved objects have low visibility (for further discussion, see Thompson et al. 2001). Visibility data can be converted into a quantitative “size” estimate by using a model for the brightness distribution and applying a Fourier transform. Since we cannot *image* the disks directly yet, we must adopt a simple empirical model capable of parameterizing the spatial extent of the disk emission.

Monnier & Millan-Gabet (2002) discuss the merits of using a “ring” model for describing the NIR emission from a circumstellar disk, based on the argument that only the hottest dust at the inner edge of the disk can contribute significantly to the NIR emission (see also Natta et al. 2001). Ring models have been fit to visibility data by other workers in the field as well (Millan-Gabet et al. 2001; Eisner et al. 2003, 2004). Furthermore, the first imaging results for the LkH α 101 disk (Tuthill et al. 2001) appear to support this class of models.

We have fitted our visibility data with a simple model consisting of a point source (representing the unresolved stellar component) and a thin (circular) ring with average diameter θ (representing the circumstellar dust emission). The thickness of the ring cannot be easily constrained for measurements on the

TABLE 1
BASIC PROPERTIES OF TARGETS

Source Names	R.A. (J2000.0)	Decl. (J2000.0)	<i>V</i> Magnitude ^a	<i>K</i> Magnitude ^a	Spectral Type ^b	Distance ^b (pc)	Adopted Luminosity ^b (L_{\odot})	Photometry References
UX Ori, HIP 23602	05 04 29.9908	-03 47 14.280	9.6	7.2	A3 (1)	460 (2)	51 ± 3 (1)	2, 3, 4, 5, 6, 7, 8, 9, 10
MWC 758, HD 36112	05 30 27.5296	+25 19 57.083	8.3	5.8	A8 V (11)	200 $^{+60}_{-40}$ (12, 13)	25 ± 4 (14)	3, 4, 7, 8, 9, 15
Z CMa A, ^c HIP 34042	07 03 43.1619	-11 33 06.209	9.9	3.8	B0 III (16)	1050 (16)	3000–310000 (16, 17)	8, 16, 18, 19
HD 58647, HIP 36068	07 25 56.0989	-14 10 43.551	6.8	5.4	B9 IVe (12, 20)	280 $^{+80}_{-50}$ (12, 13)	295 ± 50 (14)	3, 4, 7, 8, 9
HD 141569, HIP 77542	15 49 57.7489	-03 55 16.360	7.0	6.8	A0 Vev (20, 21)	99 $^{+9}_{-8}$ (12, 13)	18.5 ± 1.0 (14)	3, 4, 6, 7, 8, 9
HD 142666, v1026 Sco	15 56 40.023	-22 01 40.01	8.8	6.1	A8 Ve (20, 21, 22)	116 (22)	8.8 ± 2.5 (14)	3, 4, 6, 7, 8, 9
HD 143006, HIP 78244	15 58 33.4177	-09 00 12.174	8.4	7.1	G5 V (21)	94 ± 35 (13)	1.4 ± 0.5 (14)	3, 4, 6, 7, 8, 9, 10
HD 144432, HIP 78943	16 06 57.9575	-27 43 09.806	8.2	5.9	A9 IVev (20)	145 (23)	14.5 ± 4.0	3, 4, 6, 7, 8, 9, 10
HD 150193, MWC 863A	16 40 17.9221	-23 53 45.180	8.9	5.5	A2 IVe (20)	150 $^{+50}_{-30}$ (12, 13)	51 ± 17 (14)	2, 3, 4, 6, 7, 8, 9, 10
MWC 275, HD 163296	17 56 21.2879	-21 57 21.880	6.9	4.8	A1 Vevp (20)	122 $^{+17}_{-13}$ (12, 13)	40 ± 8 (14)	2, 3, 4, 5, 6, 7, 8, 9, 10
WW Vul, HD 344361	19 25 58.750	+21 12 31.28	10.5	7.3	A2 IVe (20)	550 (24)	65 ± 5 (1)	3, 4, 5, 6, 7, 8, 9
v1685 Cyg, MWC 340	20 20 28.2473	+41 21 51.586	10.7	5.8	B3 (1)	980 (12)	21400 ± 15000 (1)	2, 3, 4, 5, 6, 7, 8, 9
v1977 Cyg, AS 442	20 47 37.47	+43 47 24.9	10.9	6.6	B8 V (20)	700 (25)	300 ± 210 (14)	3, 4, 5, 7, 8, 9
AS 477, v1578 Cyg	21 52 34.0993	+47 13 43.612	10.2	7.2	A0 (1)	900 (26)	154 ± 20 (1)	2, 3, 4, 5, 6, 7, 8, 9

NOTE.—Units of right ascension are hours, minutes, and seconds, and units of declination are degrees, arcminutes, and arcseconds.

^a Many of the targets are variable stars and these magnitudes (*V* band from Simbad, and *K* band from 2MASS) are merely representative.

^b References are given in parentheses.

^c Z CMa is a binary system (Millan-Gabet & Monnier 2002) consisting of a Herbig component (A) and an FU Orionis star (B). The *V* and *K* magnitudes in the table are for the entire system, although our data reduction isolate the contribution from the Herbig component. The spectral type and luminosity for Z CMa A is highly uncertain (see § 4.3 for discussion).

REFERENCES.—(1) Hernández et al. 2004; (2) Hillenbrand et al. 1992; (3) Morrison et al. 2001; (4) Kharchenko 2001; (5) Morel & Magnenat 1978; (6) Gezari et al. 1999; (7) Simbad Astronomical Database; (8) 2MASS; Cutri et al. 2003; (9) Tycho-2; Høg et al. 2000; (10) DENIS Database, 2nd Release; (11) Beskrovnyaya et al. 1999; (12) van den Ancker et al. 1998; (13) Perryman (1997); (14) SED fitting, this work; (15) Joint *IRAS* Science Working Group 1988; (16) van den Ancker et al. 2004; (17) Hartmann et al. 1989; (18) Millan-Gabet & Monnier 2002; (19) Koresko et al. 1991; (20) Mora et al. 2001; (21) Dunkin et al. 1997; (22) Meus et al. 2001; (23) Pérez et al. 2004; (24) Friedemann et al. 1993; (25) Terranegra et al. 1994; (26) Lada (1985).

TABLE 2
CALIBRATOR INFORMATION

Source Name	Calibrator Name	Spectral Type	V Magnitude	K Magnitude	Adopted Uniform Disk Diameter ^a (mas)
UX Ori	HDC 33278	G9 V	8.6	6.8	0.12 ± 0.2
	HDC 36003	K5 V	7.7	4.8	0.55 ± 0.1
	HDC 26794	K3 V	8.8	6.3	0.24 ± 0.1
MWC 758	HDC 27777	B8 V	5.7	5.9	0.21 ± 0.1
	HDC 29645	G0 V	6.0	4.6	0.41 ± 0.2
Z CMa A.....	HDC 48286	F7 V	7.0	5.7	0.32 ± 0.1
	HDC 52919	K5 V	8.4	5.5	0.39 ± 0.1
	HDC 60491	K2 V	8.2	5.9	0.30 ± 0.1
HD 58647	HDC 58461	F3 V	5.8	4.9	0.39 ± 0.1
	HDC 62952	F2 V	5.0	4.2	0.39 ± 0.5
HD 141569 and HD 144432.....	HDC 139909	B9.5 V	6.9	7.0	0.16 ± 0.1
	HDC 147550	B9 V	6.2	6.3	0.21 ± 0.1
HD 142666 and HD 150193.....	HDC 144641	G3 V	8.0	6.5	0.15 ± 0.1
	HDC 134967	A2 V	6.1	6.0	0.28 ± 0.1
HD 143006	HD141107	F2 V	7.7	6.9	0.17 ± 0.1
	HD149149	G6 V	8.6	7.0	0.12 ± 0.1
MWC 275	HDC 157546	B8 V	6.3	6.5	0.17 ± 0.1
	HDC 174596	A3 V	6.6	6.5	0.21 ± 0.1
WW Vul.....	HDC 181047	G8 V	8.3	6.5	0.19 ± 0.1
	HDC 184198	F7 V	8.2	6.9	0.14 ± 0.1
v1685 Cyg and v1977 Cyg.....	HDC 199178	G2 V	7.2	5.7	0.20 ± 0.2
v1685 Cyg	HIP 102667	K2 V	8.8	6.6	0.13 ± 0.2
	HDC 192985	F5 V	5.9	4.8	0.38 ± 0.1
v1977 Cyg	SAO 50092	K0 V	8.6	6.3	0.30 ± 0.04
	HDC 199998	K2 III	8.4	5.7	0.40 ± 0.1
AS 477	HDC 201456	F8 V	7.9	6.6	0.18 ± 0.1
	HIP 109034	K4 III	9.5	6.2	0.35 ± 0.5
	HDC 199178	G2 V	7.2	5.7	0.20 ± 0.2

^a All diameter estimates were made using *getCal*, which is maintained and distributed by the Michelson Science Center (<http://msc.caltech.edu>). The diameters were estimated by fitting the spectral energy distributions with simple blackbody models.

main lobe of the visibility curve (i.e., when the fringe spacing is less than the ring diameter), and thus our results are only sensitive to the *average* ring diameter, not the ring thickness. For the fits reported here, we have used a uniform brightness ring with a fractional thickness of 20%, inspired by the LkH α 101 image.

Because our interferometer measurements lack the requisite (u , v) coverage to fully constrain our ring model, the fraction of the total K -band emission coming from the disk must be estimated separately through spectral energy distribution (SED) fitting. This method was first applied to interferometry observations of YSOs by Millan-Gabet et al. (1999) and is now in common usage (Millan-Gabet et al. 2001; Akeson et al. 2000, 2002; Eisner et al. 2003, 2004). Here we fit the broadband SED with a two-component model consisting of a stellar spectrum and a single-temperature dust blackbody. We have slightly improved on the standard procedure by using a Kurucz model (Kurucz 1979) for the underlying stellar spectrum instead of a simple blackbody, which makes some difference for sources with small IR excess or cool stellar atmospheres. Reddening of the central star must also be included in the fit, and here we adopted the reddening law from Mathis (1990); this choice affects our (dereddened) luminosity estimates for the most obscured targets.

Figure 1a shows an example of our spectral decomposition for the A8 V target HD 142666; the two-component fit is quite acceptable. From the fitting results, only two parameters are used in subsequent analysis: the K -band IR excess and the star luminosity (in cases where good literature estimates are unavailable; see Table 1). In particular, the best-fit dust temperature and flux are not directly used in visibility fitting since the ring model is purely

geometric. We note that scattered stellar light cannot be distinguished from direct stellar emission in the SED and thus the point source component might be somewhat underestimated; this effect is minimized by observing at K band, where scattering is much less efficient than for J or H bands.

Because YSOs are often variable sources, we were concerned with making reliable estimates of the K -band IR excess based on noncontemporaneous photometry. We have adopted the following procedure to conservatively estimate our observational uncertainties. We created multiple synthetic SEDs using various combinations of visible (typically, B , V , R) and infrared photometric data sets drawn from the literature. For each SED we obtained an estimate of the fraction of light at K band arising from the circumstellar dust through model fitting. The fitting results for the IR excess naturally depended on the exact photometry data used, and this variation was quantified (typically $\sim 10\%$) and reported in Table 4 for all targets. The “best estimate” was based on the SED with the most recent IR photometry (usually from the Two Micron All Sky Survey [2MASS]).

Once the NIR excess has been separately estimated, a ring model can be fit to the KI visibility data with only one free parameter, the ring diameter (having already adopted a 20% ring thickness). This process is illustrated for HD 142666 in Figure 1b, showing fitting results for three different estimates of the fraction of K -band emission coming from the dust component (“dust fraction”). Table 4 contains the complete fitting results for all sources, listing the ring diameters along with errors including both the visibility measurement error and our uncertainty in dust fraction. The reported uncertainty in the ring diameter is often

TABLE 3
KECK INTERFEROMETER VISIBILITIES

SOURCE NAME	UT DATE	PROJECTED BASELINE		VISIBILITY SQUARED ($\lambda_0 = 2.18 \mu\text{m}$, $\Delta\lambda = 0.3 \mu\text{m}$)
		U (m)	V (m)	
UX Ori	2004 Jan 7	55.547	64.015	0.483 ± 0.052
		56.336	63.635	0.476 ± 0.042
MWC 758	2002 Oct 24	50.790	67.981	0.360 ± 0.088
		49.974	68.668	0.337 ± 0.039
Z CMa A.....	2004 Apr 3	28.806	52.420	0.172 ± 0.015
	2004 Apr 5	34.159	53.142	0.186 ± 0.077
HD 58647	2004 Apr 2	30.502	49.851	0.639 ± 0.098
		27.501	49.411	0.734 ± 0.091
HD 141569	2003 Apr 17	55.224	62.474	0.978 ± 0.065
		54.102	62.180	1.056 ± 0.105
HD 142666	2004 Mar 5	56.538	58.909	0.562 ± 0.059
		56.219	56.564	0.445 ± 0.054
		55.784	55.363	0.586 ± 0.092
		55.647	55.064	0.507 ± 0.066
		53.392	51.838	0.604 ± 0.033
HD 143006	2004 Apr 2	40.097	42.871	0.931 ± 0.197
		36.677	41.635	0.863 ± 0.200
HD 144432	2003 Apr 17	54.460	49.100	0.368 ± 0.018
		54.167	48.628	0.380 ± 0.016
HD 150193	2004 Mar 5	54.858	52.468	0.205 ± 0.023
		MWC 275	2003 Apr 17	55.592
WW Vul.....	2003 Aug 9	54.449	53.157	0.218 ± 0.015
		53.189	51.683	0.218 ± 0.013
		51.713	50.306	0.232 ± 0.015
		37.683	74.410	0.642 ± 0.063
		33.914	75.528	0.558 ± 0.059
v1685 Cyg	2002 Jun 27	41.541	72.969	0.397 ± 0.069
		33.288	77.825	0.420 ± 0.108
v1977 Cyg	2002 Oct 24	45.133	69.368	0.636 ± 0.032
		34.998	76.533	0.640 ± 0.041
AS 477.....	2002 Oct 24	40.923	71.723	0.703 ± 0.025
		35.262	75.529	0.673 ± 0.054

dominated by our uncertainty in estimating the dust fraction, instead of V^2 measurement errors.

With our current single-baseline observations, we are unable to detect disk elongations if present, such as those reported by Eisner et al. (2003, 2004). Given these workers' data, we can expect up to a 50% variation in ring diameter depending on the orientation of the disk on the sky, and this source of scatter will be discussed further in § 4.1.

4. RESULTS

The results of our model fits can be found in Table 4. All but one source were resolved by the KI (the transition object HD 141569 was unresolved), and the ring diameters ranged from ~ 1.5 to 4 mas. In order to compare the ring diameters of different sources, we have converted angular diameters (milliarcseconds) into physical sizes (AU) using the estimated distances (drawn from the literature), and these values are also tabulated.

A few of our survey targets (MWC 758, HD 141569, v1685 Cyg, v1977 Cyg) were observed recently by Eisner et al. (2004) using the Palomar Testbed Interferometer (PTI). Comparing average ring diameter results, we find that PTI and KI results agree at the $1-2 \sigma$ level. This reasonable agreement suggests that neither experiment is contaminated with large-scale scattered light, since the PTI experiment has a 20 times larger field of view than the KI observations. While agreement between these two data sets is generally satisfactory, we note an apparent inconsistency

between the PTI and KI data for v1685 Cyg along one particular position angle. The current PTI data has a relatively low signal-to-noise ratio, making a definitive comparison uncertain; future work will investigate this apparent discrepancy in more detail.

4.1. Size-Luminosity Diagram

In order to investigate specific accretion disk models, we wish to compare the observed physical sizes of the NIR emission to model predictions. Since the NIR emission should be dominated by hot dust at the inner edge of the dusty disk, we expect the truncation radius to be some function of the stellar luminosity. Thus, we have plotted our results on a size-luminosity diagram (Fig. 2) using the parameters compiled in Table 1, as first described in Monnier & Millan-Gabet (2002). Since we have used a ring model for our emission geometry, the ring radius (which we measured by fitting to the visibility data) can be identified with the dust destruction radius, the location where the dust temperature exceeds the sublimation temperature.

In Figure 2 we compare our observational results to predictions of a simple physical model for the dusty circumstellar environment. Here we assume the star is surrounded by an optically thin cavity and that dust is distributed in a disk geometry at larger radii. The size of the inner cavity is set by the dust sublimation radii R_s (for sublimation temperature T_s) and can be calculated from basic radiation transfer (see the top panel of Fig. 3 for a schematic drawing). In this model, spherical dust grains at

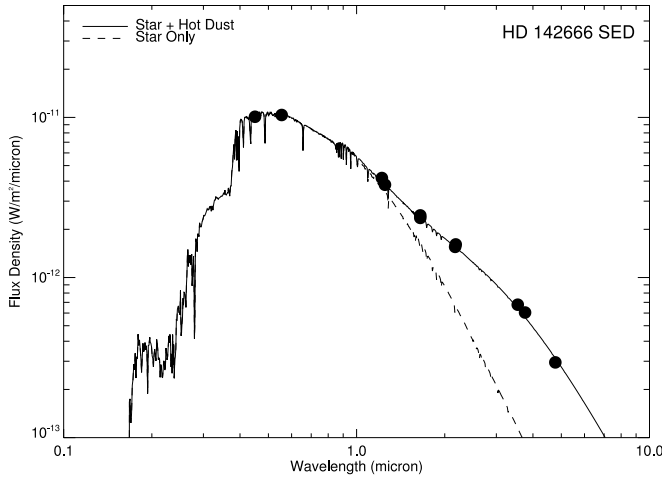


FIG. 1a

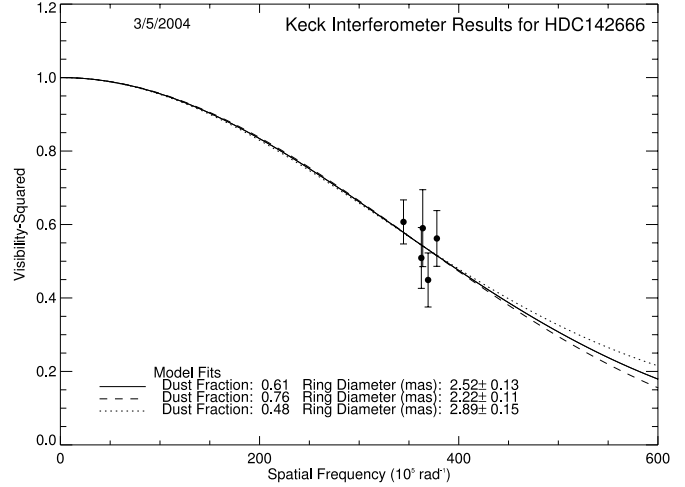


FIG. 1b

FIG. 1.—(a) SED fit for HD 142666, including (reddened) A8 V stellar spectrum plus hot dust blackbody ($T = 1355$ K). Filled circles are photometry from the *Hubble Space Telescope* Guide Star Catalog (Morrison et al. 2001), 2MASS (Cutri et al. 2003), and the Catalog of Infrared Observations (Gezari et al. 1999). (b) Ring model fits to the KI visibility data for three different estimates of the dust fraction at $2.2 \mu\text{m}$. The three dust fractions represent the range of possible values derived from the SED fitting process (see § 3).

the inner edge are in thermal equilibrium with the unobscured central star of luminosity L_* , leading to a standard result (Monnier & Millan-Gabet 2002):

$$R_s = \frac{1}{2} \sqrt{\epsilon_Q} \left(\frac{T_*}{T_s} \right)^2 R_*$$

$$= 1.1 \sqrt{\epsilon_Q} \left(\frac{L_*}{1000 L_\odot} \right)^{1/2} \left(\frac{T_s}{1500 \text{ K}} \right)^{-2} \text{ AU}, \quad (1)$$

where $\epsilon_Q = Q_{\text{abs}}(T_*)/Q_{\text{abs}}(T_s)$ the ratio of the dust absorption efficiencies $Q(T)$ for radiation at color temperature T of the incident and reemitted field, respectively.

We note that the sublimation radius derived by Dullemond et al. (2001; see their eq. [14]) is a factor of 2 times larger than equation (1), since these workers assume the dust forms an op-

tically thick “hot inner wall” at R_s . Recent work by Whitney et al. (2004) found sublimation radii close to that expected in this optically thick limit. In reality, R_s will be between these limits depending on how abruptly the dust becomes optically thick as a function of radius.

Inspection of Figure 2 reveals that Herbig targets between $1 L_\odot < L_* < 10^3 L_\odot$ have ring radii consistent with the calculated dust sublimation radii R_s for sublimation temperatures $T_s \sim 1000\text{--}1500$ K, and the observed sizes are tightly correlated with stellar luminosity. The data points in the KI size-luminosity diagram show much less scatter around the $R \propto L^{1/2}$ trend lines than was seen in previous studies (especially, Monnier & Millan-Gabet 2002). We owe the reduced scatter to the homogeneous nature of our data set and the improvements in the experimental methodology, including better target vetting for reliable spectral types, higher angular resolution, use of the K band (instead of the H band) and

TABLE 4
HERBIG Ae/Be DISK PROPERTIES

SOURCE NAME	DUST FRACTION AT K BAND ^a	RING DIAMETER	
		mas	AU
UX Ori	$0.70^{+0.08}_{-0.16}$	$2.36^{+0.43}_{-0.20}$	$1.09^{+0.20}_{-0.09}$
MWC 758	$0.72^{+0.02}_{-0.04}$	$2.75^{+0.22}_{-0.19}$	0.55 ± 0.04
Z CMa A.....	0.975 ± 0.025	3.95 ± 0.24	4.15 ± 0.25
HD 58647	$0.54^{+0.10}_{-0.04}$	2.93 ± 0.45	0.82 ± 0.13
HD 141569	0.05 ± 0.05	<20	<2
HD 142666	$0.61^{+0.15}_{-0.13}$	$2.52^{+0.41}_{-0.31}$	$0.29^{+0.05}_{-0.04}$
HD 143006	$0.53^{+0.11}_{-0.03}$	$1.63^{+1.12}_{-1.00}$	$0.15^{+0.11}_{-0.09}$
HD 144432	$0.62^{+0.02}_{-0.07}$	$3.37^{+0.32}_{-0.17}$	$0.49^{+0.05}_{-0.03}$
HD 150193	$0.67^{+0.18}_{-0.17}$	$3.84^{+1.03}_{-0.58}$	$0.58^{+0.15}_{-0.09}$
MWC 275	$0.71^{+0.07}_{-0.01}$	$3.70^{+0.14}_{-0.25}$	$0.45^{+0.02}_{-0.03}$
WW Vul.....	$0.88^{+0.03}_{-0.14}$	$1.80^{+0.24}_{-0.15}$	$0.99^{+0.13}_{-0.08}$
v1685 Cyg	$0.94^{+0.02}_{-0.09}$	$2.19^{+0.23}_{-0.18}$	$2.15^{+0.23}_{-0.18}$
v1977 Cyg	$0.94^{+0.02}_{-0.17}$	$1.61^{+0.22}_{-0.12}$	$1.13^{+0.15}_{-0.08}$
AS 477	$0.86^{+0.03}_{-0.04}$	$1.55^{+0.14}_{-0.13}$	$1.39^{+0.13}_{-0.12}$

^a Best estimate for fraction of K -band light coming from circumstellar material based on most recent photometry. Upper and lower limits are based on SED fitting to diverse data sets and represent the range of possible values given historical variability.

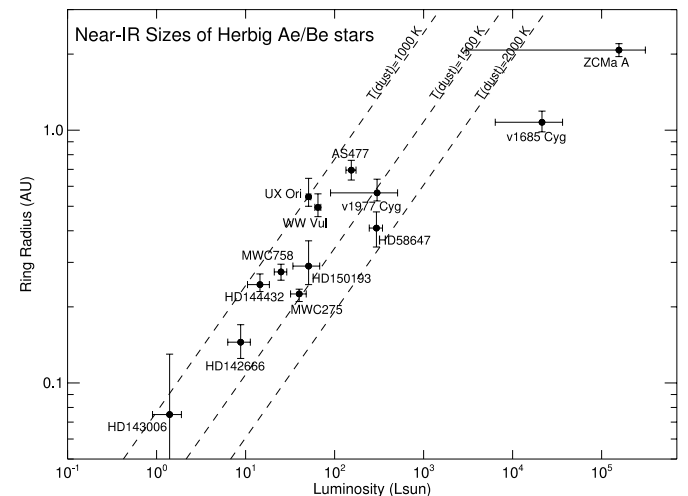


FIG. 2.—Near-infrared sizes of Herbig Ae/Be stars. The Herbig Ae/Be stars observed by the KI have been located on this “size-luminosity diagram.” The plot symbols show the radius of dust emission for the “ring” model discussed in the text. The dashed lines represent the expected inner edge of a dust disk truncated by dust sublimation at temperatures $T_s = 1000, 1500,$ and 2000 K, assuming an optically thin inner cavity and gray dust.

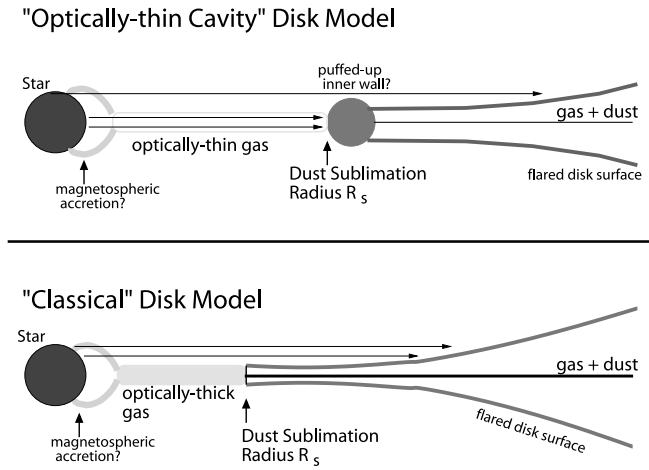


FIG. 3.—Near-infrared sizes of Herbig Ae/Be stars compared to simple models. Here we present schematics of the two disk models under consideration in this paper. *Top*: This panel shows a cross section of the inner disk region for the “optically thin cavity” model discussed in the text. *Bottom*: Here the cross section of the “classical” accretion disk model is shown. This model is nearly identical to the first, except the presence of optically thick gas in the midplane partially shields the innermost dust from stellar radiation, causing the dust sublimation radius (R_s) to shrink for the same sublimation temperature (T_s). In order to place our results in a broader context, we have labeled some additional relevant disk features (magnetospheric accretion columns, disk flaring, puffed-up inner wall) that are not directly constrained by our study. [See the electronic edition of the *Journal* for a color version of this figure.]

a smaller field of view to reject scattered light, and finally, a higher signal-to-noise ratio. These high-quality data offer definitive confirmation of the size-luminosity relations $R \propto L^{1/2}$ for Herbig Ae and late Be disks, strong evidence for the optically thin cavity model.

The remaining size scatter of about 50% is likely due to inclination effects, consistent with the range of elongations observed by Eisner et al. (2003, 2004). Further evidence for this comes from the fact that UX Ori, which is widely believed to be viewed at high inclination angle (e.g., Natta et al. 1999), is one of the most extreme targets in Figure 2, showing the lowest apparent sublimation temperature. We note that our visible-light sensitivity limit ($R \lesssim 10.5$) introduces a bias against edge-on sources if the disk heavily obscures the star.

We appreciate that the true NIR brightness distribution of YSO disks may not be adequately described by the ring model adopted here, despite our sound scientific motivations. Only future imaging work by IOTA, CHARA, and/or VLTI interferometers will unambiguously establish the true emission geometry. However, regardless of the exact emission morphology, the size-luminosity trends presented here should still remain valid if the targets in our sample share a common emission geometry.

4.2. “Undersized” Disks around High-Luminosity Sources

While the “optically thin cavity” model can explain the observed sizes of Herbig Ae and late Be stars, the higher luminosity (high- L) sources clearly deviate from the model predictions. These measured disk sizes are many times too small to be consistent with the size-luminosity relations found for the lower luminosity sources. While our sample only contains two such sources, v1685 Cyg (B3) and Z CMa A (B0?), the results must be taken seriously given the unambiguous discrepancy that cannot be explained by known sources of uncertainty (however, see § 4.3 for specific discussion of the problematic Z CMa system).

In order to investigate this further, we have calculated the dust sublimation radii for an alternate disk model: the “classical”

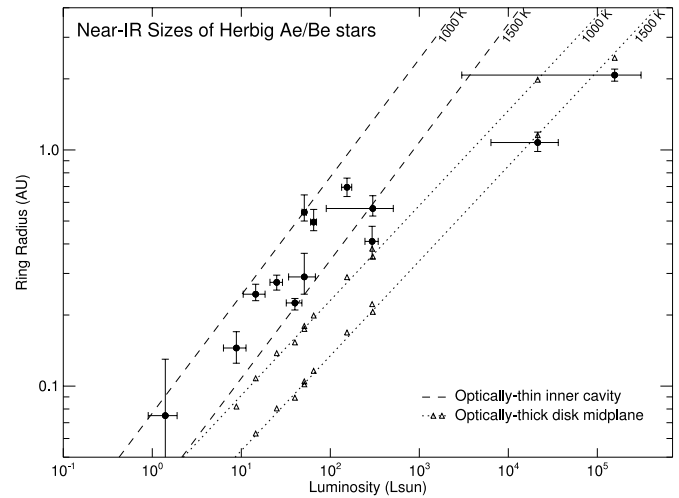


FIG. 4.—Size-luminosity diagram here allows one to compare the observed disk sizes (filled circles) with the predictions of two simple disk models (see Fig. 3). The dashed lines show the disk sizes, assuming an optically thin inner disk (same as Fig. 2), while the dotted lines show mean relations for the inner dust radius predicted for an optically thick, geometrically thin inner disk model (open triangles show calculation for individual sources). Both models assume gray dust, and results are shown for dust sublimation temperatures $T_s = 1500$ and 1000 K. Note that if the inner wall of the “optically thin cavity” model is truly opaque, as proposed by Dullemond et al. (2001), then the inferred sublimation temperatures are larger by ~ 500 K (see § 4.1 for more discussion).

optically thick, geometrically thin disk model for $T_s \sim 1500$ and 1000 K (e.g., Hillenbrand et al. 1992; Millan-Gabet et al. 2001). The main difference from the previous model is that a thin disk of gas acts to shield the dusty disk from direct stellar illumination. Thus, the expected sublimation radii R_s are significantly smaller than for the corresponding optically thin cavity model. Figure 3 contains a sketch contrasting the two model geometries under investigation here.

The dust destruction radius for the classical accretion disk model is not a pure function of luminosity (see above references for derivation of analytical formulation), and thus a separate model estimate must be made for each target based on specific stellar parameters. The results of this calculation are plotted in Figure 4 along with the KI disk sizes and the previously derived size-luminosity relations (e.g., eq. [1]). Here we see that the high- L targets are fit better by “classical” accretion disk models than by the optically thin cavity models, confirming the recent analysis of Eisner et al. (2004) based on v1685 Cyg, MWC 1080, and MWC 297.

We can look for further confirmation of this trend by reconsidering the results of Monnier & Millan-Gabet (2002). These authors also found many high- L disks to have “undersized” emission, although a few notable targets showed *order-of-magnitude* larger sizes than their high- L peers. Notably, MWC 349 and LkH α 101 (targets resolved by aperture masking) were much larger than their counterparts measured with long-baseline interferometry. Perhaps these sources represent more evolved systems where strong stellar winds have either cleared the inner disk of gas or photoevaporation has eroded the inner disk. Regardless, our KI results reveal a population of high-luminosity YSOs with disk sizes much smaller than possible for models with optically thin inner cavities.

In summary, our new KI data support the conclusions of previous studies that some high-luminosity (early Herbig Be) stars show evidence for significant gaseous inner disks. There appears to be a diversity of such disks, from those consistent with

completely optically thick disk midplanes (Eisner et al. 2004; this work) to those with intermediate-tau inner cavities (perhaps optically thick only in the ultraviolet; see Monnier & Millan-Gabet 2002). We note that dust destruction radii data alone cannot directly constrain the geometry of the inner gaseous material—a completely optically thick midplane has a similar effect to an intermediate-tau spherical gas distribution. In order to distinguish between these scenarios, one must incorporate other observations that also probe the inner accretion disk, such as *mid-infrared* disk sizes (e.g., recently reported by Hinz et al. 2001; Leinert et al. 2004), H α spectropolarimetry (Vink et al. 2002), and high-resolution spectroscopy of the molecular gas (e.g., Najita et al. 2003; Brittain et al. 2003; Blake & Boogert 2004).

4.3. Comments on Individual Sources

HD 141569.—HD 141569, the only unresolved target in our survey, is thought to be in a transition stage between pre-main-sequence disk and debris disk. Although disk structures can be seen in scattered light (Clampin et al. 2003), SED modeling by Li & Lunine (2003) and others suggests that nearly all the NIR emission is from the star and that the disk emits significant radiation only at longer wavelengths. Our own SED-fitting and KI data support this picture.

UX Ori.—UX Ori is the prototype of pre-main-sequence objects showing deep visual minima interpreted as obscuration by dust clouds. UXOR behavior is thought to arise for YSOs (typically Herbig Ae/Be stars) that are viewed at high inclination (e.g., Natta et al. 1999), such that our line of sight partially intercepts the accretion disk. Under these conditions, we expect the simple “ring” emission geometry (assumed here for visibility fitting) to break down. As we discussed in § 4.1, UX Ori has a relatively large disk size, showing a deviation from the mean size-luminosity relations of Figure 2. The NIR emission of UX Ori is likely not ringlike, and we may be seeing scattered light if the inner disk emission is partially obscured by the outer flared disk. Clearly, UX Ori is a prime target for interferometric imaging with VLTI and CHARA.

HD 58647.—According to Figure 2, this disk is unusually small considering its luminosity. In fact, it has the hottest inferred dust sublimation temperature of the low-luminosity Herbig stars. Recently, Manoj et al. (2002) argued that this source is more likely a classical Be star rather than a pre-main-sequence object. Indeed, if the NIR emission is partly arising from free-free (gas) emission, we would expect the observed interferometric size to be small.

Z CMa.—This binary source consists of a Herbig (Z CMa A) and an FU Orionis object (Z CMa B) in a close (~ 100 mas) orbit (e.g., Garcia et al. 1999; Koresko et al. 1991). The KI was able to observe both sources independently using the 50 mas resolution of the adaptive optics system (the FU Orionis component will be treated in R. Millan-Gabet et al. 2005, in preparation). Determining the photometric contributions of the two components separately is problematic because of strong variability and the small angular separation.

This source is also highly embedded (Hartmann et al. 1989; Whitney et al. 1993), and thus the applicability of the “ring model” for describing the NIR emission is suspect. In addition, the spectral type and luminosity of the Herbig component is highly uncertain—with a factor of 100 in luminosity separating two reasonable estimates. We adopt a lower limit of $3000 L_{\odot}$ here based on the bolometric luminosity of the system (Hartmann et al. 1989), while an upper limit of $310,000 L_{\odot}$ comes from dereddening an assumed B0 III spectral type (van den Ancker

et al. 2004). Obviously this large luminosity uncertainty makes definitive analysis of the KI data impossible, and we encourage follow-up spectroscopic and interferometric observations to confirm the properties of this unique and challenging source.

5. CONCLUSIONS

We have definitively measured the near-infrared size-luminosity relations for disks around Herbig Ae/Be stars for $L_* < 10^3 L_{\odot}$. Valid over more than two decades in stellar luminosity L , the NIR sizes obey the simple scaling relation $R \propto L^{1/2}$. This relation is predicted by the “optically thin cavity” model for YSO disks (Tuthill et al. 2001; Natta et al. 2001; Monnier & Millan-Gabet 2002), and our results imply dust sublimation temperatures in the expected range of $T_s \sim 1000\text{--}1500$ K.

In contrast, the infrared sizes of circumstellar disks for the high-luminosity sources in our sample ($L_* > 10^3 L_{\odot}$) are more consistent with *optically thick* inner disks, supporting recent conclusions of Eisner et al. (2004). Significant gas in the inner disk midplane could explain these observational results, although the gas spatial distribution is not *directly* constrained here. Exceptions to this trend are notable (LkH α 101 and MWC 349, reported elsewhere), perhaps signaling the clearing of the inner gaseous disk by the strong stellar winds and ionizing radiation from evolved O and early B stars.

Future work will progress on two fronts, one theoretical and the other observational. We will focus on using state-of-the-art physical models to fit SEDs and visibilities at both near-IR and mid-IR wavelengths. Such work will allow us to move beyond merely qualitative tests of new disk models (e.g., the DDN models; Dullemond et al. 2001), for instance by quantifying the optical depth and geometry of the inner gaseous disk. These studies will provide the density and temperature profiles needed for studies of planet formation.

To advance observationally, more single-baseline data are still needed for classical T Tauri disks (R. L. Akeson et al. 2005, in preparation), for FU Orionis stars (R. Millan-Gabet et al. 2005, in preparation), and for the highest luminosity sources. In contrast, studies of Herbig Ae disks will not be significantly advanced with more single-baseline data, given the (now) large body of existing results; Herbig Ae disks should now be *imaged* to make additional progress. With closure phase imaging from IOTA, VLTI, and/or CHARA interferometers, we will test predictions of the next-generation of *physical* models, such as those incorporating a “puffed-up inner wall” (Dullemond et al. (2001).

The authors wish to thank the all members of the Keck Interferometer development team (JPL, MSC, WMKO), whose dedicated efforts made this “shared risk” commissioning science possible. This material is based upon work supported by NASA under JPL contracts 1236050 and 1248252 issued through the Office of Space Science. Data presented herein were obtained at the W. M. Keck Observatory from telescope time allocated to the National Aeronautics and Space Administration through the agency’s scientific partnership with the California Institute of Technology and the University of California. The Observatory was made possible by the generous financial support of the W. M. Keck Foundation. This research has made use of the SIMBAD database, operated at CDS, Strasbourg, France. This publication makes use of data products from the Two Micron All Sky Survey (2MASS), which is a joint project of the University

of Massachusetts and the Infrared Processing and Analysis Center/California Institute of Technology, funded by the National Aeronautics and Space Administration and the National Science Foundation. This work has made use of services produced by the Michelson Science Center at the California Institute

of Technology. The authors wish to recognize and acknowledge the very significant cultural role and reverence that the summit of Mauna Kea has always had within the indigenous Hawaiian community. We are most fortunate to have the opportunity to conduct observations from this mountain.

REFERENCES

- Adams, F. C., Lada, C. J., & Shu, F. H. 1987, *ApJ*, 312, 788
- Akeson, R. L., Ciardi, D. R., van Belle, G. T., & Creech-Eakman, M. J. 2002, *ApJ*, 566, 1124
- Akeson, R. L., Ciardi, D. R., van Belle, G. T., Creech-Eakman, M. J., & Lada, E. A. 2000, *ApJ*, 543, 313
- Akeson, R. L., et al. 2005, *ApJ*, in press
- Beskrovnaya, N. G., et al. 1999, *A&A*, 343, 163
- Blake, G. A., & Boogert, A. C. A. 2002, *ApJ*, 606, L72
- Brittain, S. D., Rettig, T. W., Simon, T., Kulesa, C., DiSanti, M. A., & Dello Russo, N. 2003, *ApJ*, 588, 535
- Calvet, N., Patino, A., Magris, G. C., & D'Alessio, P. 1991, *ApJ*, 380, 617
- Chiang, E. I., & Goldreich, P. 1997, *ApJ*, 490, 368
- Clampin, M., et al. 2003, *AJ*, 126, 385
- Colavita, M. M. 1999, *PASP*, 111, 111
- Colavita, M. M., & Wizinowich, P. L. 2000, *Proc. SPIE*, 4006, 310
- . 2003, *Proc. SPIE*, 4838, 79
- Colavita, M., et al. 2003, *ApJ*, 592, L83
- Cutri, R. M., et al. 2003, *2MASS All Sky Catalog of Point Sources (Pasadena: JPL)*
- Danchi, W. C., Tuthill, P. G., & Monnier, J. D. 2001, *ApJ*, 562, 440
- Dullemond, C. P., Dominik, C., & Natta, A. 2001, *ApJ*, 560, 957
- Dunkin, S. K., Barlow, M. J., & Ryan, S. G. 1997, *MNRAS*, 286, 604
- Eisner, J. A., Lane, B. F., Akeson, R. L., Hillenbrand, L. A., & Sargent, A. I. 2003, *ApJ*, 588, 360
- Eisner, J. A., Lane, B. F., Hillenbrand, L. A., Akeson, R. L., & Sargent, A. I. 2004, *ApJ*, 613, 1049
- Friedemann, C., Riemann, H. G., Gurtler, J., & Toth, V. 1993, *A&A*, 277, 184
- Garcia, P. J. V., Thiébaud, E., & Bacon, R. 1999, *A&A*, 346, 892
- Gezari, D. Y., Pitts, P. S., & Schmitz, M. 1999, *Catalog of Infrared Observations (5th ed.; Strasbourg: CDS)*
- Hartmann, L., Kenyon, S. J., & Calvet, N. 1993, *ApJ*, 407, 219
- Hartmann, L., Kenyon, S. J., Hewett, R., Edwards, S., Strom, K. M., Strom, S. E., & Stauffer, J. R. 1989, *ApJ*, 338, 1001
- Hernández, J., Calvet, N., Briceño, C., Hartmann, L., & Berlind, P. 2004, *AJ*, 127, 1682
- Hillenbrand, L. A., Strom, S. E., Vrba, F. J., & Keene, J. 1992, *ApJ*, 397, 613
- Hinz, P. M., Hoffmann, W. F., & Hora, J. L. 2001, *ApJ*, 561, L131
- Høg, E., et al. 2000, *A&A*, 355, L27
- Joint *IRAS* Science Working Group. 1988, *IRAS Point Source Catalog, Ver. 2 (NASA PR-1190; Washington: NASA)*
- Kharchenko, N. V. 2001, *Kinemat. Phys. Celest. Bodies*, 17, 409
- Koresko, C. D., Beckwith, S. V. W., Ghez, A. M., Matthews, K., & Neugebauer, G. 1991, *AJ*, 102, 2073
- Kuchner, M. J., & Lecar, M. 2002, *ApJ*, 574, L87
- Kurucz, R. L. 1979, *ApJS*, 40, 1
- Lada, C. J. 1985, *ARA&A*, 23, 267
- Leinert, C., et al. 2004, *A&A*, 423, 537
- Li, A., & Lunine 2003*ApJ*, 594, 987
- Lynden-Bell, D., & Pringle, J. E. 1974, *MNRAS*, 168, 603
- Manoj, P., Maheswar, G., & Bhatt, H. C. 2002, *MNRAS*, 334, 419
- Mathis, J. S. 1990, *ARA&A*, 28, 37
- Meeus, G., Waters, L. B. F. M., Bouwman, J., van den Ancker, M. E., Waelkens, C., & Malfait, K. 2001, *A&A*, 365, 476
- Michelson, A. A., & Pease, F. G. 1921, *ApJ*, 53, 249
- Millan-Gabet, R., & Monnier, J. D. 2002, *ApJ*, 580, L167
- Millan-Gabet, R., Schloerb, F. P., & Traub, W. A. 2001, *ApJ*, 546, 358
- Millan-Gabet, R., Schloerb, F. P., Traub, W. A., Malbet, F., Berger, J. P., & Bregman, J. D. 1999, *ApJ*, 513, L131
- Monnier, J. D., & Millan-Gabet, R. 2002, *ApJ*, 579, 694
- Mora, A., et al. 2001, *A&A*, 378, 116
- Morel, M., & Magnenat, P. 1978, *A&AS*, 34, 477
- Morrison, J. E., Röser, S., McLean, B., Bucciarelli, B., & Lasker, B. 2001, *AJ*, 121, 1752
- Najita, J., Carr, J. S., & Mathieu, R. D. 2003, *ApJ*, 589, 931
- Natta, A., Prusti, T., Neri, R., Thi, W. F., Grinin, V. P., & Mannings, V. 1999, *A&A*, 350, 541
- Natta, A., Prusti, T., Neri, R., Wooden, D., Grinin, V. P., & Mannings, V. 2001, *A&A*, 371, 186
- Pérez, M. R., van den Ancker, M. E., de Winter, D., & Bopp, B. W. 2004, *A&A*, 416, 647
- Perryman, M. A. C. 1997, *The Hipparchos and Tycho Catalogues (ESA Sp-1200; Noordwijk: ESA)*
- Shao, M., & Staelin, D. H. 1977, *J. Opt. Soc. Am. A*, 67, 81
- Swain, M., et al. 2003, *ApJ*, 596, L163
- Terranegra, L., Chavarria-K., C., Diaz, S., & Gonzalez-Patino, D. 1994, *A&AS*, 104, 557
- Thompson, A. R., Moran, J. M., & Swenson, G. W. 2001, in *Interferometry and Synthesis in Radio Astronomy*, ed. A. R. Thompson et al. (2nd ed.; New York: Wiley), 692
- Tuthill, P. G., Monnier, J. D., & Danchi, W. C. 2001, *Nature*, 409, 1012
- van den Ancker, M. E., Blondel, P. F. C., Tjin A Djie, H. R. E., Grankin, K. N., Ezhkova, O. V., Shevchenko, V. S., Guenther, E., & Acke, B. 2004, *MNRAS*, 349, 1516
- van den Ancker, M. E., de Winter, D., & Tjin A Djie, H. R. E. 1998, *A&A*, 330, 145
- Vink, J. S., Drew, J. E., Harries, T. J., & Oudmaijer, R. D. 2002, *MNRAS*, 337, 356
- Whitney, B. A., Clayton, G. C., Schulte-Ladbeck, R. E., Calvet, N., Hartmann, L., & Kenyon, S. J. 1993, *ApJ*, 417, 687
- Whitney, B. A., Indebetouw, R., Bjorkman, J. E., & Wood, K. 2004, *ApJ*, 617, 1177
- Wizinowich, P. L., Le Mignant, D., Stomski, P. J., Acton, D. S., Contos, A. R., & Neyman, C. R. 2003, *Proc. SPIE*, 4839, 9

ERRATUM: “THE NEAR-INFRARED SIZE-LUMINOSITY RELATIONS
FOR HERBIG Ae/Be DISKS” (ApJ, 624, 832 [2005])

J. D. MONNIER, R. MILLAN-GABET, R. BILLMEIER, R. L. AKESON, D. WALLACE, J.-P. BERGER, N. CALVET,
P. D’ALESSIO, W. C. DANCHI, L. HARTMANN, L. A. HILLENBRAND, M. KUCHNER, J. RAJAGOPAL,
W. A. TRAUB, P. G. TUTHILL, A. BODEN, A. BOOTH, M. COLAVITA, J. GATHRIGHT,
M. HRYNEVYCH, D. LE MIGNANT, R. LIGON, C. NEYMAN, M. SWAIN,
R. THOMPSON, G. VASISHT, P. WIZINOWICH, C. BEICHMAN,
J. BELETIC, M. CREECH-EAKMAN, C. KORESKO,
A. SARGENT, M. SHAO, AND G. VAN BELLE

Because of an error at the Press, the received date for this paper was incorrectly given as 2004 January 5. The correct received date is 2004 December 5. The Press sincerely regrets this error.